

X-ray specular reflectivity and anomalous scattering in the vicinity of the Si *K* absorption edge in quartz

J. M. André and A. Maquet

Laboratoire de Chimie Physique, Université Pierre et Marie Curie, 11 rue Pierre et Marie Curie, F-75231 Paris Cédex 05, France*

R. Barchewitz

Laboratoire de Chimie Physique, Université Pierre et Marie Curie, and Laboratoire pour l'Utilisation du Rayonnement Electromagnétique (L.U.R.E.), Université de Paris-Sud, F-91405 Orsay Cédex, France*

(Received 22 June 1981)

X-ray specular reflectivity of quartz has been measured at various grazing angles as a function of the frequency in the vicinity of the *K*-absorption edge of silicon. An anomalous behavior in the spectral distribution of the continuous reflected intensity is observed accompanying a maximum in the photoabsorption spectrum. The optical constants are deduced from the measured reflectivity coefficients. We present a simple theoretical approach which enables us to account for the experimental results.

I. INTRODUCTION

It has been recognized for several years that the x-ray reflectivity of crystals, under Bragg conditions, may exhibit pronounced anomalous variations at frequencies close from a critical frequency of the material.^{1,2} More recently a similar behavior has been also observed in the case of x-ray specular reflection from mirrors under grazing incidence.³⁻⁶ Since the reflectivity may be expressed in terms of the coherent anomalous scattering amplitude which, in turn, is related to the absorption coefficient, it appears that such measurements can provide interesting indications on the inner-shell absorption spectra of the reflecting material. However, given the limitations of conventional sources, there were, up to now, relatively few applications. The advent of powerful synchrotron sources, which has led to a renewal of interest in those areas, should radically change the situation.^{7,8}

The goal of this paper is to show that specular x-ray reflectivity measurements can be revealed as extremely useful for obtaining absolute determinations of the optical constants (and ultimately of the scattering factors) in the anomalous regions when other methods are inadequate or insufficiently accurate. For the sake of illustration of the method, we present here absolute measurements of the specular reflectivity of quartz at frequencies close to the *K*-absorption edge of silicon.

Our choice was motivated by the fact that the spectral distribution reflected from a quartz monocrystal, under Bragg conditions, presents several interesting structures. In particular a characteristic feature consisting of a pronounced maximum, has been ob-

served since the early works by Cauchois and Bonnelle,² and Heno.⁹ Recent experimental absorption spectra in the same frequency range were obtained by Sénémaud and Costa-Lima,¹⁰ for both amorphous and crystalline SiO₂. Thus it seemed of interest to compare the data obtained from these different methods, since such results can provide useful information on the electronic structure of these compounds.¹¹

The organization of the paper is as follows: Sec. II is devoted to a brief exposition of the relations existing between specular x-ray reflectivity and forward Rayleigh scattering. An approximate theoretical approach, valid in the immediate vicinity of a critical absorption frequency is exposed in Sec. III. The experimental measurements are presented and analyzed in Sec. IV. Section V is constituted by a brief discussion of our results.

II. X-RAY SPECULAR REFLECTIVITY AND SCATTERING

In the visible range, the specular reflectivity *R* for a nonabsorbing medium is given by the Fresnel formula in terms of the real Drude refractive index *n_D*. For instance, at normal incidence, assuming an unpolarized radiation

$$R = \left(\frac{n_D - 1}{n_D + 1} \right)^2 \quad (1)$$

In the x-ray range, absorption cannot be neglected anymore and it is customary to merely replace the Drude index *n_D* by the complex quantity

$n_D^* = n_D - ix_D$ as a simple transposition from the visible range optics.¹² The quantity x_D , called the extinction coefficient, is directly related to the linear absorption coefficient μ of the medium at the wavelength λ via the well-known optical theorem $x_D = \lambda\mu/4\pi$. Actually a more careful analysis,¹³ shows that such a simple approach is inadequate and that specular x-ray reflection should be consistently treated as a boundary value problem for an electromagnetic wave reaching a homogeneous, isotropic, and absorbing medium.

Assuming the medium is separated from the vacuum by a smooth surface, the reflectivity for an unpolarized beam becomes

$$R = \frac{1}{2}(r_{\parallel}r_{\parallel}^* + r_{\perp}r_{\perp}^*) \quad (2)$$

where $r_{\parallel}, r_{\parallel}^*$ and r_{\perp}, r_{\perp}^* are the Fresnel coefficients and their conjugates for, respectively, the parallel and perpendicular components with respect to the incidence plane. Under an oblique incidence, an analysis taking into account the heterogeneity of the waves propagating within the absorbing medium leads to the following expressions¹⁴:

$$r_{\perp} = \frac{\sin u - a + ix}{\sin u + a - ix}; \quad (3a)$$

$$r_{\parallel} = -\frac{(\epsilon' \sin u - a) - i(\epsilon'' \sin u - x)}{(\epsilon' \sin u + a) - i(\epsilon'' \sin u + x)}, \quad (3b)$$

where u is the glancing angle, ϵ' and ϵ'' are, respectively, the real and imaginary parts of the complex dielectric constant ϵ . The so-called heterogeneity parameter a is connected to the real part of the complex refractive index $n^* = n - ix$ via

$$a = n \cos \theta, \quad (4)$$

where θ is the angle between the equi-amplitude and the equiphase planes.

All these quantities are related to the complex Drude, refractive index $n_D^* = n_D - ix_D$ through the complex dielectric constant $\epsilon = \epsilon' - i\epsilon''$:

$$\epsilon' = n_D^2 - x_D^2; \quad (5a)$$

$$\epsilon'' = 2n_D x_D; \quad (5b)$$

and

$$2n^2 = [(\epsilon' - \cos^2 u)^2 + \epsilon''^2]^{1/2} + \cos^2 u + \epsilon'; \quad (6a)$$

$$2x^2 = [(\epsilon' - \cos^2 u)^2 + \epsilon''^2]^{1/2} + \cos^2 u - \epsilon'; \quad (6b)$$

$$2a^2 = [(\epsilon' - \cos^2 u)^2 + \epsilon''^2]^{1/2} - \cos^2 u + \epsilon'. \quad (6c)$$

In the above relations (5), it is implicitly assumed that the magnetic permeability of the medium is unity, which is usually verified in the x-ray range. The above expressions provide the sought after relations between the specular reflectivity and the complex Drude refractive index which can be evaluated from the well-known relation:

$$n_D^* = 1 + 2\pi r_0 \left(\frac{c}{\omega}\right)^2 \sum_i N_i F_i(\omega), \quad (7)$$

where N_i stands for the number of scatterers i per unit volume, r_0 is the classical radius of the electron, and $F_i(\omega)$ is the forward Rayleigh scattering amplitude for the scatterer i .

III. ANOMALOUS SCATTERING AMPLITUDE

Exact calculation of the second-order scattering amplitude is not a simple job even in the naive case of a nonrelativistic hydrogenic atom.¹⁵ Extension to the relativistic domain represents a formidable task.¹⁶ Useful approximate calculations based on the hydrogenic model have been nevertheless performed following Hönl's method. For an account of recent works along these lines see the paper by Wagenfeld.¹⁷

Extension to more realistic self-consistent atomic models, including relativistic contributions, were presented together with extensive tabulations by Cromer and Liberman.¹⁸ These data have been widely used in the literature on anomalous scattering and represent, to the best of our knowledge, the more accurate theoretical computations of the continuum contributions to the anomalous scattering factor. The principle of such calculations lies on the fact that the real and imaginary parts of $F(\omega)$ are connected, via the dispersion relations, to the photoelectric cross section. A common limitation of these results is that they are valid only in the nonresonant case, i.e., far from the absorption edge. We present here a simple semiphenomenological approach which does not suffer from such a drawback.

The dimensionless transition amplitude $F(\omega)$ for forward Rayleigh scattering of photons of energy $\hbar\omega$ and polarization $\vec{\epsilon}$ on an atomic electron in the state denoted $|0\rangle$ of energy E_0 is¹⁹

$$F(\omega) = -m\omega^2 \sum_n |\langle n | \vec{r} \cdot \vec{\epsilon} | 0 \rangle|^2 \left[\frac{1}{E_0 - E_n + \hbar\omega + \frac{1}{2}i\Gamma_n} + \frac{1}{E_0 - E_n - \hbar\omega + \frac{1}{2}i\Gamma_n} \right], \quad (8)$$

where $\vec{r} \cdot \vec{\epsilon}$ represents the dipole interaction operator, and the infinite sum runs over the complete set of excited states $|n\rangle$ of energy E_n , belonging either to a discrete or to a continuous spectrum.

Since we are interested in anomalous scattering in the vicinity of a characteristic absorption frequency, we have modified the usual Kramers-Heisenberg formula by introducing the widths Γ_n of the states $|n\rangle$. Obviously those

widths are of relevance only in resonant or quiresonant conditions. Note that, for computational convenience, we have used the $\vec{E} \cdot \vec{r}$ form of the dipole interaction operator instead of $\vec{A} \cdot \vec{p} + A^2$. Both representations are known to be equivalent if the phenomenological widths Γ_n are discarded. The inclusion of these latter leads to minor corrections which can be safely neglected within the order of approximation retained here.²⁰

When averaged over the polarization directions of the incoming photons and after introducing the oscillator strength $g_{n,0} = (2m/\hbar)\omega_{n,0}|\langle n|x|0\rangle|^2$, where $\omega_{n,0} = (E_n - E_0)/\hbar$, the amplitude $F(\omega)$ is conveniently rewritten

$$F(\omega) = \frac{1}{2}\omega^2 \sum_n \frac{g_{n,0}}{\omega_{n,0}} \left(\frac{1}{\omega_{n,0} - \omega - i\Gamma_n/2\hbar} + \frac{1}{\omega_{n,0} + \omega - i\Gamma_n/2\hbar} \right). \quad (9)$$

Then, one gets easily the usual formal expressions of the real and imaginary parts of the amplitude

$$\text{Re}F(\omega) = \frac{1}{2}\omega^2 \sum_n \frac{g_{n,0}}{\omega_{n,0}} \left(\frac{\omega_{n,0} - \omega}{(\omega_{n,0} - \omega)^2 + (\Gamma_n/2\hbar)^2} + \frac{\omega_{n,0} + \omega}{(\omega_{n,0} + \omega)^2 + (\Gamma_n/2\hbar)^2} \right), \quad (10a)$$

$$\text{Im}F(\omega) = \frac{1}{2}\omega^2 \sum_n \frac{g_{n,0}}{\omega_{n,0}} \frac{\Gamma_n}{2\hbar} \left(\frac{1}{(\omega_{n,0} - \omega)^2 + (\Gamma_n/2\hbar)^2} + \frac{1}{(\omega_{n,0} + \omega)^2 + (\Gamma_n/2\hbar)^2} \right). \quad (10b)$$

It should be stressed that a complete calculation of the scattering amplitude $F(\omega)$ as it stands would meet with considerable difficulties since every process contributing to the decay of the excited states (radiative processes, autoionization, Auger transitions, etc.) should be consistently included in the calculation of the widths Γ_n .⁸ Obviously such a treatment is beyond the scope of our paper; instead we shall generalize a more pragmatic approach, initially proposed by Bremer *et al.*,⁴ which, although extremely simplified, will enable us to interpret the experimental results. The main features of the method are summarized in the following.

The calculation is performed within the dipole approximation. Such an approximation may seem to be questionable in the domain of frequency considered here, i.e., in the vicinity of the K edge of silicon ($\lambda \sim 6,7 \text{ \AA}$). However, as noted by Wagenfeld,²¹ higher multipoles contributions affect principally angular distributions. In the case of forward scattering, we are interested in, those contributions would amount at most to a few percents and consequently are discarded. Similarly relativistic contributions are neglected. Such a limitation is consistent with our choice of the dipole approximation since relativistic corrections would be of the same order of magnitude as multipolar ones.²² As another approximation we have adopted a one-electron model. Such an approach is fairly well justified in resonant and nearly resonant conditions since other electrons, which do not participate directly in the process, only contribute to an almost constant background.

It is well known that the absorption spectrum of quartz at the silicon K edge presents a typical "white line."^{2,10} As expected, the specular reflectivity presents a corresponding anomalous behavior in the same domain of frequency.³ See Fig. 2 below. On the basis of these experimental results one is led to

the following assumptions: in the anomalous region the infinite sum entering the expression of $F(\omega)$ is split into two contributions corresponding, respectively, to the so-called white line and to the continuous spectrum. As an additional simplifying hypothesis we shall suppose that the white line has a Lorentzian shape and that the distribution of oscillator strengths in the continuum follows a simple inverse-power law. Such a simplified picture corresponds to describe the absorption spectrum in this region as the combination of a Lorentzian line and a typical \tan^{-1} edge. Note that the width of the Lorentzian can be estimated from independent measurements and the characteristic parameters governing the shape of the edge may be deduced from reasonable theoretical assumptions concerning, in particular, the core-hole lifetime.

A. "White line" contribution

The analysis is standard in this case since the infinite sum entering Eqs. (10a) and (10b) is reduced to the contribution of the resonant (or quiresonant) state $|n\rangle$ directly coupled to the initial state by the radiation field. Accordingly the second, nonresonant, term in those expressions can be safely discarded. Then, one recovers the usual dispersion formulas for a Lorentzian absorption line:

$$\text{Re}F_w(\omega) \simeq \frac{1}{2}\omega^2 \frac{g_{n,0}}{\omega_{n,0}} \frac{\omega_{n,0} - \omega}{(\omega_{n,0} - \omega)^2 + (\Gamma_{n/0}/2\hbar)^2}; \quad (11a)$$

$$\text{Im}F_w(\omega) \simeq \frac{1}{2}\omega^2 \frac{\Gamma_{n/0}}{2\hbar} \frac{g_{n,0}}{\omega_{n,0}} \frac{1}{(\omega_{n,0} - \omega)^2 + (\Gamma_{n/0}/2\hbar)^2}, \quad (11b)$$

where the index "w" stands for white line. Note that using instead a Breit-Wigner-Fano analysis should not affect significantly the results of the following discussion.

B. Contribution of the continuum of states

The contribution of the transitions towards the continuum of states lying above the absorption edge is evaluated as follows: (a) Above the q edge the density of oscillator strengths $dg/d\omega$ is assumed to follow a simple inverse power law in terms of the frequency²³:

$$\left(\frac{dg}{d\omega}\right)_q = \begin{cases} g_q \frac{\alpha-1}{\omega_q} \left(\frac{\omega_q}{\omega}\right)^\alpha & \text{if } \omega \geq \omega_q \\ 0 & \text{if } \omega < \omega_q \end{cases} \quad (12a)$$

$$(12b)$$

$$\operatorname{Re}F_c(\omega) = \left(\frac{\omega}{\omega_q}\right)^2 g_q \frac{\alpha-1}{2} \int_{\omega_q}^{\infty} d\omega' \left(\frac{\omega_q}{\omega'}\right)^{\alpha+1} \left[\frac{\omega'-\omega}{(\omega'-\omega)^2 + (\Gamma/2\hbar)^2} + \frac{\omega'+\omega}{(\omega'+\omega)^2 + (\Gamma/2\hbar)^2} \right], \quad (13a)$$

$$\operatorname{Im}F_c(\omega) = \left(\frac{\omega}{\omega_q}\right)^2 g_q \frac{\alpha-1}{2} \frac{\Gamma}{2\hbar} \int_{\omega_q}^{\infty} d\omega' \left(\frac{\omega_q}{\omega'}\right)^{\alpha+1} \left[\frac{1}{(\omega'-\omega)^2 + (\Gamma/2\hbar)^2} - \frac{1}{(\omega'+\omega)^2 + (\Gamma/2\hbar)^2} \right], \quad (13b)$$

where the index c stands for the continuum contribution.

Integrals similar to those entering Eqs. (13a) and (13b) are usually evaluated in closed form by using contour integration.^{4,23} This leads to cumbersome calculations especially when α is different from an integer (or a half integer). Instead we found convenient to express them in terms of Gauss hypergeometric functions ${}_2F_1(a, b; c; z)$.²⁴ This goal is conveniently achieved via the change of variable $u = \omega_q/\omega'$. The typical integral

$$J_\alpha(\omega_q, \omega) = \int_{\omega_q}^{+\infty} d\omega' \left(\frac{\omega_q}{\omega'}\right)^\alpha \left[(\omega'-\omega)^2 + \left(\frac{\Gamma}{2\hbar}\right)^2 \right]^{-1} \quad (14)$$

is accordingly transformed as follows:

$$J_\alpha(\omega_q, \omega) = \omega_q^{-1} \int_0^1 du u^\alpha (1-zu)^{-1} (1-z^*u)^{-1}, \quad (15)$$

where $z = (\omega + i\Gamma/2\hbar)/\omega_q$. Then

$$J_\alpha(\omega_q, \omega) = z \left(\frac{i\Gamma}{\hbar}\right)^{-1} \int_0^1 du u^\alpha (1-zu)^{-1} + \text{c.c.} \quad (16)$$

The remaining integral represents a Gauss hypergeometric function²⁴

$$J_\alpha(\omega_q, \omega) = z (i\Gamma/\hbar)^{-1} (\alpha+1)^{-1} \times {}_2F_1(1, \alpha+1; \alpha+2; z) + \text{c.c.} \quad (17)$$

After some algebra using, in particular, contiguity relations between functions whose parameters differ by

where the index q denotes the shell of the initial state, ω_q is the corresponding threshold frequency, g_q is the total oscillator strength associated with the transition and α is an adjustable parameter, which value depends on the shell considered and verifying the inequalities $2.5 \leq \alpha < 3$.

(b) One assumes that the widths Γ_n (or the lifetimes) of the excited states belonging to the continuum are constants $\Gamma_n \simeq \Gamma$, the magnitude of Γ being essentially governed by the width of the core hole. Again, our choice of Γ will be justified in Sec. IV.

The above assumptions lead to the following expressions:

one unit, one gets the following general expressions:

$$\operatorname{Re}F_c(\omega) = \left(\frac{\omega}{\omega_q}\right)^2 g_q \frac{\alpha-1}{4(\alpha+1)} \times [{}_2F_1(1, \alpha+1; \alpha+2; z) + {}_2F_1(1, \alpha+1; \alpha+2; -z) + \text{c.c.}] \quad (18a)$$

$$\operatorname{Im}F_c(\omega) = i \left(\frac{\omega}{\omega_q}\right)^2 g_q \frac{\alpha-1}{4(\alpha+1)} \times [{}_2F_1(1, \alpha+1; \alpha+2; z) - {}_2F_1(1, \alpha+1; \alpha+2; -z) - \text{c.c.}] \quad (18b)$$

In the particular cases $\alpha=3$ and $\frac{5}{2}$, which are relevant, respectively, for the contribution of the K shell and the $L_{II}, L_{III}, M_I, \dots$ shells,²³ one can recover the usual expressions, through the use of the relations

$${}_2F_1\left(1, \frac{1}{2}; \frac{3}{2}; t^2\right) = 1/2t \ln \left| \frac{1+t}{1-t} \right|$$

or

$${}_2F_1\left(1, \frac{1}{2}; \frac{3}{2}; -t^2\right) = 1/t \tan^{-1}t$$

and

$${}_2F_1(1, 1; 2; -t) = 1/t \ln(1+t)$$

together with the contiguity relation²⁴

$${}_2F_1(1, \alpha+1; \alpha+2; t) = \frac{\alpha+1}{\alpha} t^{-1} [{}_2F_1(1, \alpha; \alpha+1; t) - 1]$$

Our results generalize and extend in a straightforward way those previously obtained by using Kramers-Krönig dispersion relations connecting the real and imaginary parts of the scattering amplitude via integral relations. By contrast with ours, such an approach leads naturally to use contour integration.^{4,25} In particular we are not compelled to introduce fictitious absorption coefficients for negative frequencies as Bremer did.⁴ Another interesting feature of the expressions (18a) and (18b) is that the hypergeometric functions involved have their parameter $a = 1$. Consequently they have a continued-fraction expansion converging into the whole complex plane except on the cut $(+1, +\infty)$.²⁶

IV. EXPERIMENTS AND RESULTS

A. Experimental

The essential features of the experimental setup are shown in Fig. 1. The incident continuous radiation is provided by the Anneau de Collisions d'Orsay (ACO) storage ring operated at its maximum energy (540 MeV, 100 mA). The beam is successively reflected by two pairs of parallel plane mirrors and then analyzed by a vacuum bent-crystal spectrograph.²⁷

Both mirrors of the first pair are coated with a thin evaporated chromium film. They are used as low pass filter to suppress higher energies which could be selectively reflected in higher orders by the bent-crystal analyzer.²⁸ In fact, when the synchrotron is operated on its maximum energy the intensity radiated at 3.35 \AA is about 15% of that radiated at our working wavelength of 6.7 \AA . We have checked that the half-wavelength component was practically cut off at a glancing angle of $u = 18 \text{ mrad}$. Under such conditions the available intensity at 6.7 \AA is reduced by only 40%.

The second pair of reflectors consists of the sample mirror and a gold plated mirror. After reflection on the latter the beam recovers its original direction. The sample is a monocrystal of quartz, optically polished along the $10\bar{1}0$ reticular planes. The reflectivity

of every mirror, but the sample, presents no anomalous behavior in the considered energy range. The spectral distribution of the specularly reflected radiation is analyzed near the K edge of silicon with a 020 gypsum, 250-mm radius, bent crystal, oriented in the first order of selective reflection with a Bragg angle $\phi = 26^\circ$. The detector is a KODAK SA3 photographic emulsion for which the blackening curves have been established. The film is stored into a box where it can be automatically wound off under vacuum for each exposure. As the effective aperture of the crystal is about 15 mm, the spectral range analyzed covers approximately 200 eV.

B. Reflectivity spectra

Figures 2(b)–2(c) show the microdensitograms of the spectral distribution observed at various glancing angles. Since the incident radiation distribution is perfectly uniform [Fig. 2(a)], the pronounced fluctuations can be attributed without ambiguity to the specular reflection on the quartz sample. The shape of the reflected radiation distribution appears to be different according to whether the glancing angle is smaller or higher than $u \approx 12 \text{ mrad}$.

Below this value, the distribution presents a dip 1 on the lower-energy side reaching a minimum 2 looking like a narrow white line on the film. It should be noted that the dip 1 is located at an energy very close from the K -absorption discontinuity of the silicon. At higher energies one observes two features 4_1 and 4_2 embedded within a wide plateau. The reflected intensity then increases steadily in 5 until reaching the average level of the distribution. Note that the secondary features 4_1 and 4_2 are not observed with a glass mirror containing a high proportion of amorphous SiO_2 . This enables us to conclude that they are characteristic of the crystalline structure of the sample.

Beyond $u \sim 12 \text{ mrad}$ [Figs. 2(c)–(e)], on the high-energy side of the white line 2, a maximum of intensity 3 shows up, looking like a "black line" on the film. Its relative intensity increases with the glancing angle u . Simultaneously the slope of the dip 1 becomes less steep on the lower-energy side. Ulti-

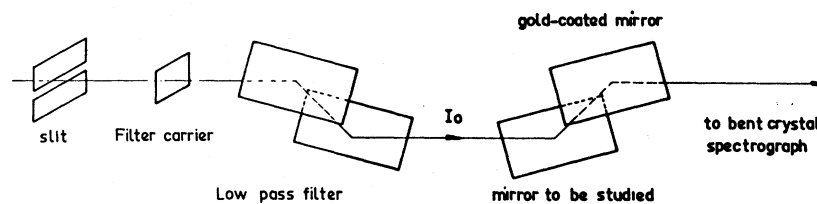


FIG. 1. Scheme of the experimental setup.

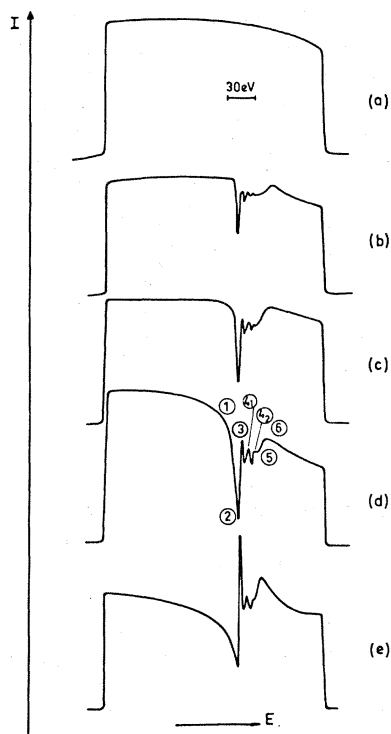


FIG. 2. Spectral distribution of the specularly reflected radiation on a quartz crystal, optically polished along the 1010 planes, in the vicinity of the Si K -absorption threshold ($E_K = 1840$ eV). (b)–(e) are spectra obtained at various glancing angles u : (b) $u = 9$ mrad; (c) $u = 12$ mrad; (d) $u = 15$ mrad; (e) 20 mrad. (a) displays the spectral distribution of the incident beam. The curves are smoothed densitograms.

mately a broad feature appears in 6.

For the sake of comparison we present also (Fig. 3) the absorption spectrum obtained by transmission through a fine powder of quartz.² This spectrum presents the same general features than specular reflectivity at small glancing angles.

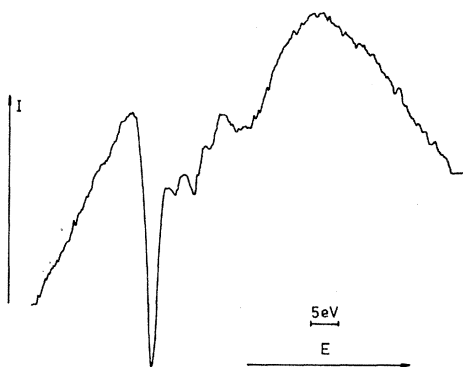


FIG. 3. Absorption spectrum obtained by transmission through a fine powder of quartz (Ref. 2). (Courtesy of Professor Cauchois and Professor Bonnelle.)

C. Determination of the optical constants

From the measurement of the absolute value of the reflectivity at different glancing angles, the Drude optical constants n_D and x_D can be simultaneously derived at a given frequency. We have carried out such absolute measurements in the energy range ~ 1820 – 1875 eV.

As the final value of the refractive index may be strongly affected by a small variation of the reflectivity it is essential to determine the relative precision of our measurements of the reflected intensity. Broadly speaking one can distinguish between two kinds of sources of uncertainties corresponding, respectively, to the principle of the measurement and to the detection technique, i.e., the use of photographic films.

Belonging to the first category is the fact that after the reflection on the quartz sample the x-ray beam is again reflected on the gold-coated mirror before being analyzed. It is thus necessary to extract the contribution of this latter mirror in order to determine precisely the quartz reflectivity. For this purpose, we have replaced the quartz sample by another gold-coated mirror, during a new set of intensity measurements. Another important parameter is the incident intensity I_0 reaching the film: I_0 is directly proportional to a visible component of the source and thus can be determined with great accuracy. Note also that the reflectivity depends through the relations (3)–(6), on the glancing angle u which in some cases cannot be determined within a precision better than 0.3 mrad.

The other source of uncertainty which should be analyzed is the photographic detection device. The blackening curves have been systematically established after each set of measurements by recording the primary intensity $I_0(\omega)$ reaching the film. The obtained curves fit the usual semiempirical law of the following general form:

$$\ln(e^d - 1) = \gamma \ln I_0(\omega) t - b, \quad (19)$$

where d is the optical density, $I_0(\omega)$ the intensity, t is the exposure time, and γ and b are adjustable parameters. The absolute accuracy on the optical density depends on the densitometric method used and can be evaluated in standard ways. Given the high intensity of the ACO radiation the exposure time t may be very short (typically 12–20 sec) so that the relative error may become significant. The error on the parameter γ is negligible: the processing conditions do not alter the contrast since the films are simultaneously treated. Finally it is more difficult to evaluate the accuracy on the parameter b which depends in a complicated way on the wavelength through the spectral distribution of the incident radiation, the analyzer reflectivity and the response of the emulsion.

A careful analysis of the sources of errors for each

run, i.e., at each glancing angle, shows that the confidence level of our experimental results is better than 20%. Note that such an accuracy compares very favorably with standard absorption spectroscopy measurements.²⁹

In order to reduce the effect of the above experimental errors (including possible systematic ones) on computed values of the optical constants we have introduced, at each glancing angle, a correcting factor acting on the product $I_0(\omega)t$ in formula, Eq. (19). This factor has been determined by comparing the measured reflectivity R far from the absorption edge (for instance at $\lambda = 7 \text{ \AA}$) with a theoretical value obtained on using the classical Kallmann-Mark formula for the real part of the refractive index n_D and the recent semiempirical data given by Leroux *et al.*,²⁹ for the linear absorption coefficients μ . Depending on the glancing angle the relative correction is comprised between 5 and 20%.

The dependence of the Drude optical constants of the medium in terms of the energy has been determined from the variations of the corrected reflectivity in terms of both the energy and the glancing angle u . The actual computation has been carried out by using a standard optimization procedure. At a given energy, one chooses an arbitrary value for one of the constants x_D or n_D . Then the value of the other one is deduced from the corrected reflectivity at each glancing angle. The computation is then reiterated until the variance is found minimum. Note that such calculations can be carried out successfully only for glancing angles lower than the average critical value $u_c = \sqrt{2\delta}$, where $\delta = 1 - n_D$, since beyond this value

the reflectivity changes very slowly in terms of the ratio x_D/n_D .

The dependence of the experimental values of the decrement $\delta = 1 - n_D$ and of the linear photoabsorption coefficient μ , in terms of the energy, are shown in the Fig. 4. Note that the typical features, whose magnitude depends on the glancing angle u , observed into the reflection spectrum are in some sense "translated" into the dispersion curves of δ and μ . This point will be considered further into Sec. V. Note also that our absolute values of μ are in good agreement with experimental values obtained from glassy SiO_2 by transmission, in particular at the maximum of absorption: $\mu_{\text{max}} \approx 8000 \text{ cm}^{-1}$.¹⁰

V. DISCUSSION

The observed behavior of the quartz specular reflectivity near the Si K -absorption edge results from the strong anomalous dispersion of the refractive index in this region. It corresponds also to the pronounced absorption maximum responsible for the typical white line observed in the transmission spectrum. The connection between both phenomena is made clear by using the simple theoretical approach presented in Sec. III. As already mentioned the calculation is split into two contributions corresponding, respectively, to the white line and to the continuous spectrum.

A. White line contribution

The absorption line results from a transition between the Si $1s$ level and orbitals with a strong Si $3p$ character into the conduction band.

In the absence of any reliable theoretical data we used a Lorentzian fit of the absorption line,^{10,30} in order to determine the parameters entering the expression of $\text{Re}F_w(\omega)$ and $\text{Im}F_w(\omega)$, Eqs. (11a) and (11b). We obtained in that way the relevant values of the width ($\Gamma \approx 2.2 \text{ eV}$) and of the height of the maximum, corresponding to the oscillator strength of the transition.

B. Continuous spectrum contribution

We used the values of Cromer's tabulations for the oscillator strengths. The widths Γ , relative to the Si K shell, are assumed to be equal to the width of the silicon K hole. We used the values tabulated by Sevier.³¹ The general expressions Eqs. (13a) and (13b) have been specialized to the case $\alpha = 3$, following the common use for the K shell. Note that, in this particular case, they can be written under the simpler form

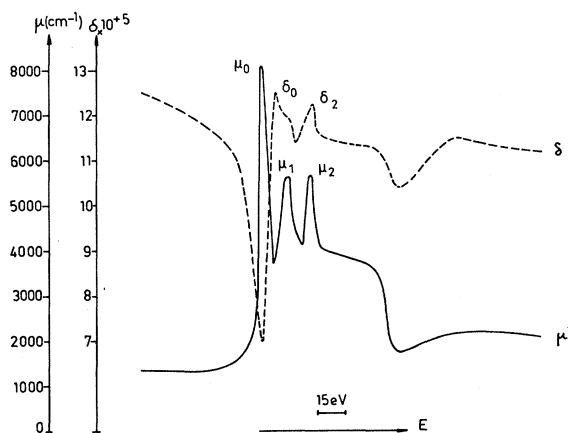


FIG. 4. Variations of the decrement δ and the absorption coefficient μ deduced from the corrected experimental values of the reflectivity.

$$\operatorname{Re}F_c(\omega) \approx -g_K \left[1 + \frac{1}{2} \left(\frac{\omega_K}{\omega} \right)^2 \left\{ \ln \left[\left(\frac{\omega - \omega_K}{\omega_K} \right)^2 + \left(\frac{\Gamma_K}{2\hbar\omega_K} \right)^2 \right] + \ln \left[\left(\frac{\omega + \omega_K}{\omega_K} \right)^2 + \left(\frac{\Gamma_K}{2\hbar\omega_K} \right)^2 \right] \right\} \right]; \quad (20a)$$

$$\operatorname{Im}F_c(\omega) \approx g_K \left(\frac{\omega_K}{\omega} \right)^2 \left[\tan^{-1} \left(\frac{\omega + \omega_K}{\Gamma_K/2\hbar} \right) - \tan^{-1} \left(\frac{\omega - \omega_K}{\Gamma_K/2\hbar} \right) \right]. \quad (20b)$$

We have included the contributions from other electronic levels of silicon and oxygen and verified that they amount to an almost constant background.

The variations of the theoretical values of the optical constants $\delta = 1 - n_D$ and μ are plotted in Figs. 5. One can verify that the shapes of the theoretical and experimental curves are similar. In particular the

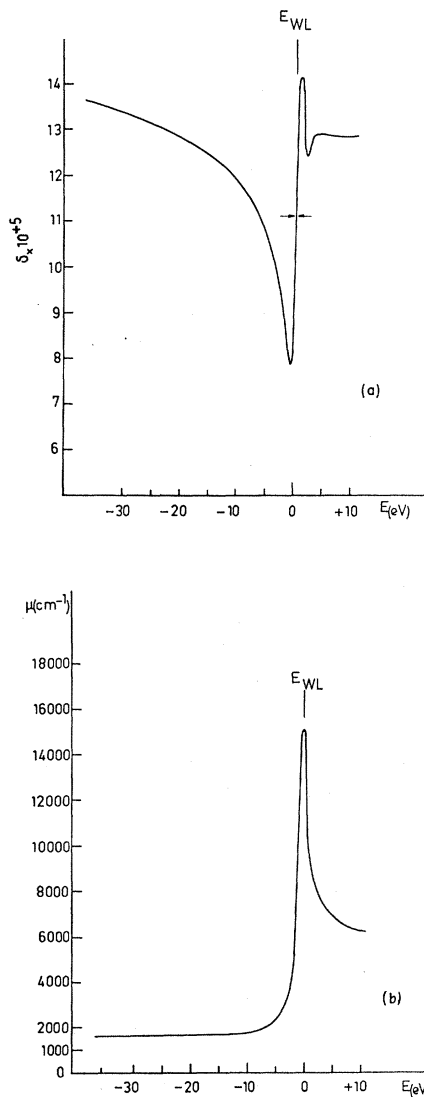


FIG. 5. Theoretical dispersion curves for the decrement δ (a) and the absorption coefficient μ (b).

values of the decrement δ are in good agreement. However, the theoretical values of the linear absorption coefficient μ are systematically higher than those derived from our reflectivity measurements. This discrepancy results probably from the fact that Cromer's theoretical values of the atomic Si K oscillator strength are not exactly suited to the description of transitions in SiO_2 .

Finally, from those values of the Drude optical constants we have computed the corresponding reflectivity R . The dependence of R on the glancing angle u reproduces fairly well the experimental distribution of the reflected radiation (Figs. 6).

The relations existing between the optical constants δ and μ may be easily established since those quantities are connected via the Kramers-Kronig dispersion relations. Schematically an isolated maximum in the μ distribution induce a corresponding maximum, slightly shifted towards higher energies, in the δ distribution. This situation is clearly exemplified when comparing the features μ_2 and δ_2 (Figs. 5). Note however that when two maxima are close enough in the μ distribution the corresponding features in the δ distribution may coalesce. Thus, the complex feature noted δ_0 , corresponds to the maxima μ_0 and μ_1 (Figs. 5).

The interpretation of the reflectivity distribution is

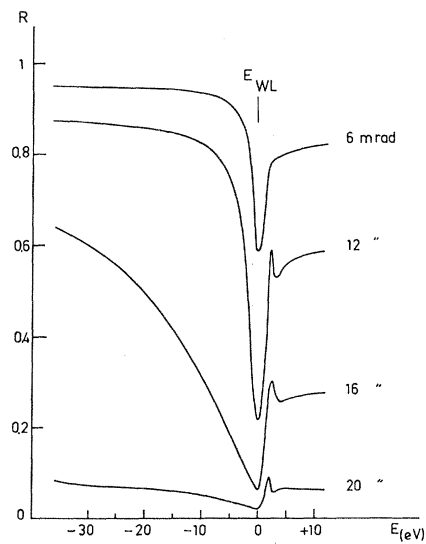


FIG. 6. Theoretical variations of the reflectivity at various glancing angles.

much more involved. As a matter of fact R depends in a complicated way of μ , δ , and u . The general behavior of R may be nevertheless connected to that of δ . For instance, a δ maximum induces a maximum in the reflectivity spectrum. This can be ascribed to the fact that any steep variation of δ , modifies accordingly the critical angle $u_c = \sqrt{2\delta}$ which in turns, depending on the glancing angle, affects the reflectivity R . However, this change is modulated by the corresponding variations of μ so that the behavior of R depends in fact on the respective magnitude of the maxima present in the δ and μ distributions. This latter remark holds in particular for describing secondary structures such that 4_1 , 4_2 (Figs. 3) or extended x-ray absorption fine structure (EXAFS).

As a final comment we wish to point out that the method we presented here compares very favorably with others for precise determination of the optical

constants and even of the scattering factor of a medium. The only limitation comes from the need for high quality mirrors in order to minimize the diffuse scattering which lowers the sensitivity of the method. In particular the state of the surface, including previous treatments, should be recorded in order to compare the experimental results with other ones provided by different techniques. If those prerequisites are satisfied the measurement of x-ray specular reflectivity represents a useful way of investigation of inner-shell spectra, specially when standard methods are inadequate. Note also that scattering factors can be determined in that way, even in glassy or amorphous samples.

One of us (R.B.) gratefully thanks the staff of the ACO storage ring for its assistance. We thank also R. Marmoret who kindly checked most of the theoretical computations.

*Laboratoire associé au CNRS.

¹Y. Cauchois, C. R. Acad. Sci. (Paris) **242**, 100 (1956).

²Y. Cauchois and C. Bonnelle, C. R. Acad. Sci. (Paris) **242**, 1596 (1956).

³R. Barchewitz, C. Bonnelle, R. Cremonese, and G. Onori, C. R. Acad. Sci. (Paris) **268B**, 151 (1969); C. Bonnelle and R. Barchewitz, in *Proceedings of the International Conference on the Physics of X-Ray Spectra*, edited by R. D. Deslattes (NBS, Gaithersburg, Maryland, 1976). See also R. Barchewitz, thesis (Université Pierre et Marie Curie, Paris, 1977) (unpublished).

⁴J. Bremer, L. Kaihola, and R. Keski-Kuha, J. Phys. C **13**, 2225 (1980).

⁵L. Kaihola and J. Bremer, J. Phys. C **14**, L43 (1981).

⁶J. M. André and R. Barchewitz, Solid State Commun. **38**, 489 (1981).

⁷A comprehensive survey of recent applications of synchrotron radiation may be found in *Synchrotron Radiation Research*, edited by H. Winnick and S. Doniach (Plenum, New York, 1980).

⁸G. Wendin, Phys. Scr. **21**, 535 (1980).

⁹H. Heno, C. R. Acad. Sci. (Paris) **242**, 1599 (1956).

¹⁰C. Sénémaud and M. T. Costa-Lima, in *The Physics of SiO₂ and its Interfaces*, edited by S. T. Pantelides (Pergamon, New York, 1978); and (private communication).

¹¹D. L. Griscom, J. Non-Cryst. Solids **24**, 155 (1977).

¹²J. A. Prins, Z. Phys. **46**, 755 (1928).

¹³B. L. Henke, Phys. Rev. A **6**, 94 (1972).

¹⁴M. R. Lefevre and M. Montel, Opt. Acta **20**, 97 (1973).

¹⁵One may use compact representation of the Coulomb Green's function. See for instance, M. Gavrilu, Phys. Rev. **163**, 147 (1967); Z. Phys. A **293**, 269 (1979). Y. Heno, A. Maquet, and R. Schwarcz, J. Appl. Phys. **51**, 11 (1980).

¹⁶G. E. Brown, R. E. Peierls, and J. B. Woodward, Proc. R. Soc. London Ser. A **227**, 59 (1954).

¹⁷H. Wagenfeld, in *Anomalous Scattering*, edited by S. Ramaseshan and S. C. Abrahams (Munksgaard, Copenhagen, 1975), p. 13.

¹⁸D. T. Cromer and D. Liberman, J. Chem. Phys. **53**, 1891 (1970). See also D. T. Cromer, Acta Crystallogr. **18**, 17 (1965).

¹⁹J. J. Sakurai, *Advanced Quantum Mechanics* (Addison-Wesley, Reading, Mass., 1977).

²⁰J. M. André, thesis (Université Pierre et Marie Curie, Paris, 1981) (unpublished).

²¹H. Wagenfeld, Phys. Rev. **144**, 216 (1966).

²²M. S. Jensen, Phys. Lett. **74A**, 41 (1979); J. Phys. B **13**, 4337 (1980).

²³L. G. Paratt and C. F. Hempstead, Phys. Rev. **94**, 1593 (1954).

²⁴*Higher Transcendental Functions*, Bateman Manuscript Project, edited by A. Erdelyi (McGraw-Hill, New York, 1953), Vol. 1.

²⁵T. Kawamura and T. Fukamachi, Jpn. J. Appl. Phys. **17**, 224 (1978).

²⁶H. S. Wall, *Analytic Theory of Continued Fractions* (Chelsea, New York, 1973).

²⁷R. Barchewitz, C. Bonnelle, and Y. Cauchois, in *Proceedings of the International Symposium for Synchrotron Radiation Users*, edited by G. V. Marr and I. M. Munro (Daresbury, 1973), p. 311.

²⁸R. Barchewitz, M. Montel, and C. Bonnelle, C. R. Acad. Sci. (Paris) B **264**, 363 (1967).

²⁹J. Leroux and T. P. Thinh, in *Revised Tables of X-Ray Mass Absorption Coefficients*, edited by Claisse Scientific Corp. (Quebec, 1977).

³⁰P. S. Wei and F. W. Lytle, Phys. Rev. B **19**, 679 (1979), and references therein.

³¹K. D. Sevier, *Low Energy Electron Spectrometry* (Wiley, New York, 1972).